Volume 1 | Number 1 | Jan 2013 | Pages 1–100

PCCP

Physical Chemistry Chemical Physics
www.rsc.org/pccp

ROYAL SOCIETY OF CHEMISTRY

ROYAL SOCIETY OF CHEMISTRY

www.rsc.org/pccp

ARTICLE TYPE

Stress in titania nanoparticles: An atomistic study

Robert Darkins[a], **Maria L. Sushko**[b], **Jun Liu**[b], and **Dorothy M. Duffy**[*a]

Stress engineering is becoming an increasingly important method for controlling electronic, optical, and magnetic properties of nanostructures, although the concept of stress is poorly defined at the nanoscale. We outline a procedure for computing bulk and surface stress in nanoparticles using atomistic simulation. The method is applicable to ionic and non-ionic materials alike and may be extended to other nanostructures. We apply it to spherical anatase nanoparticles ranging from 2 to 6 nm in diameter and obtain a surface stress of 0.89 N/m, in agreement with experimental measurements. Based on the extent that stress inhomogeneities at the surface are transmitted into the bulk, two characteristic length-scales are identified: below 3 nm bulk and surface regions cannot be defined and the available analytic theories for stress are not applicable, and above about 5 nm the stress becomes well-described by the theoretical Young-Laplace equation. The effect of a net surface charge on the bulk stress is also invesigated. It is found that moderate surface charges can induce significant bulk stresses, on the order of 100 MPa, in nanoparticles within this size range.

1 Introduction

Stress is a physical quantity that expresses the forces that neighbouring atoms exert on each other. It is well-defined in continuum mechanics but loses its rigour in the atomic limit. Nevertheless, stress is very important at the atomic scale and plays an essential role in the properties of nanomaterials.

Stress modifies the electronic band structure of materials[1–5] which, in turn, modifies the electronic, optical, and magnetic properties. This behaviour has wide-ranging applications. For example, lattice mismatches are often exploited in the design of semiconductor heterostructures[6–8]. The lattice mismatch produces strain that either alters the band gap directly or, if the stresses are too large to be tolerated, results in the generation of misfit dislocations to ease the strain[5]. The optical properties of silicon nanoparticles have also been engineered through strain by embedding them in a host matrix[9].

Many of the exceptional properties of decahedral gold nanoparticles are attributed to the large stresses that result from the disclination intrinsic to their five-fold structure[10,11]. The strain energy is also believed to play an important part in their poorly-understood stability and morphology[12,13].

It has even been reported that the surface stress intrinsic to metal nanowires can be sufficiently large to induce phase transformations in the bulk[14,15].

A continuum-based approach to stress in nanomaterials will often be inadequate, omitting details that only emerge in an atomistic treatment[16]. However, despite the importance of stress in nanomaterials design, there have been no previous atomistic studies of stress in nanostructures of multi-component materials, such as metal oxides. This is not due to a lack of theoretical groundwork[17–25] but is likely due to

the challenges of computing local stress in such materials. When the standard techniques for computing local stress are applied to multi-component materials they produce unphysical answers. Indeed, the only atomistic studies that we are aware of that investigate local stress in nanostructures have all been limited to one-component metals (*e.g.,* Refs[26–32]). It was only in a recent paper by Branicio and Srolovitz that a set of methods for handling atomic-level stress specifically in multi-component materials were outlined[33]. One of the easier-to-implement and more versatile of these methods, and that refined in this work, combines the standard virial stress computation with Hardy's[34] idea of locally smearing the atoms in space. To our knowledge, the present work provides the first practical application of this method.

Titania nanoparticles are one of the most ubiquitous nanomaterials, with several important technological applications[35], including photocatalysis, sensors, solar cells, and memory devices. Accordingly, their size-dependent stress/strain properties have received a considerable amount of experimental attention[36–41]. Of particular interest is the paper of Zhang, Chen and Banfield[36] in which X-ray diffraction was used to determine the size-dependent lattice parameters of nanoparticles as small as 4 nm (a size readily accessible to simulation). From the lattice parameters the bulk strain and stress, and thence the surface stress, were determined. The nanoparticles were of the anatase polymorph and were shown using transmission electron microscopy to be very nearly spherical, a consequence of the high temperatures at which they were grown. In the present paper we outline a procedure, applicable to any material, for computing both bulk and surface stress in nanoparticles. When applied to anatase we achieve excellent agreement with the measurements of
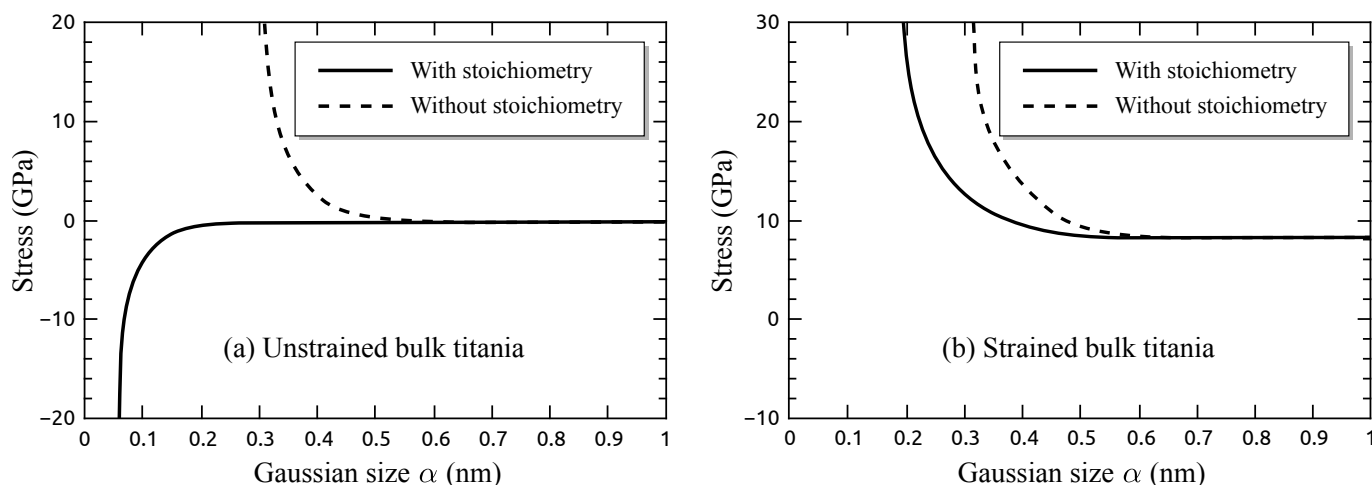
Fig. 1 The $\frac{1}{3}\mathrm{Tr}(\mathbf{\Pi})$-stress in bulk titania averaged over all titanium ions for a range of Gaussian sizes. Without the stoichiometric correct, Equation (1) is used, and with, Equation (3). In (a) the titania is unstrained, and in (b) the titania was strained by 5% in the [001] direction.

Zhang et al[36]. Further to this, the effect of charge on the bulk stress of nanoparticles is investigated. An example application of charged nanoparticles is in the construction of thin films *via* the self-assembly of nanoparticles that have been oppositely charged (*e.g.,* through amine-functionalisation)[42,43].

2 Results and Discussion

2.1 Atomic-level stress

A continuous atomic-level stress field $\Pi^{\alpha\beta}(\mathbf{r})$ can be computed through local spatial averaging of the atomic virials. Branicio and Srolovitz[33] proposed to achieve this by convoluting the atomic virial tensors $\mathscr{W}_i^{\alpha\beta}$ with a normalized localisation function $\mathscr{P}(\mathbf{r})$, *viz.*

$$\Pi^{\alpha\beta}(\mathbf{r}) = \sum_i \mathscr{P}(\mathbf{r} - \langle \mathbf{r}_i \rangle)\langle \mathscr{W}_i^{\alpha\beta}\rangle \qquad (1)$$

where we sum over each atom i in the system, and $\langle \cdot \rangle$ denotes time-averaging. A justification for this equation and the expression for $\mathscr{W}_i^{\alpha\beta}$ are both provided in the Methodology section below. In this work we employ a Gaussian localisation function

$$\mathscr{P}(\mathbf{r}) = \frac{27}{\alpha^3(2\pi)^{3/2}}\exp(-9r^2/2\alpha^2) \qquad (2)$$

where α parametrizes the size of the Gaussian and is equivalent to three standard deviations.

In multi-component materials the atomic virials exhibit large, unphysical, species-dependent modulations. In which case, too small a choice of α will result in large and unphysical variations in the stress field that obfuscates the true Cauchy

stress field, while too large a value will impede the resolution. The ideal choice of α would therefore be the smallest value that achieves a smooth, converged stress field.

Convergence of the stress field occurs at any given point once the virial contributions from the local ions approach the correct stoichiometry. Generalising Eq. 12 of Ref[33], we propose a modification to Equation (1) that involves scaling the ionic contributions so as to artificially achieve the correct stoichiometry for smaller choices of α,

$$\Pi^{\alpha\beta}(\mathbf{r}) = \sum_X \mathscr{S}_X(\mathbf{r})\sum_{i\in X}\mathscr{P}(\mathbf{r} - \langle \mathbf{r}_i \rangle)\langle \mathscr{W}_i^{\alpha\beta}\rangle \qquad (3)$$

where we sum over all species X and all atoms $i \in X$ belonging to species X, and have introduced the stoichiometric correction

$$\mathscr{S}_X(\mathbf{r}) = \frac{\sum_j \mathscr{P}(\mathbf{r} - \langle \mathbf{r}_j \rangle)}{\sum_{j\in X}\mathscr{P}(\mathbf{r} - \langle \mathbf{r}_j \rangle)}\frac{n_X}{\sum_Y n_Y} \qquad (4)$$

where n_X equals the number of atoms X in the material formula (*e.g.,* for TiO_2, $n_{Ti} = 1$ and $n_O = 2$).

To identify an appropriate α and test the efficacy of the stoichiometric correction, we averaged the hydrostatic ($\frac{1}{3}\mathrm{Tr}(\mathbf{\Pi}(\mathbf{r}))$) stress at the sites of the titanium ions within a bulk slab of anatase for $\alpha \in (0,1)$ nm, with and without the stoichiometric correction, and for two cases: i) unstrained anatase, and ii) anatase that had been strained by 5% in the [001] direction. The results are plotted in Figure 1(a) and (b), respectively. In both cases the stoichiometric correction accelerates convergence, although not as significantly in the strained case. Clearly for anatase a suitable, and somewhat conservative, Gaussian size would be $\alpha = 0.5$ nm with the stoichiometric correction included. We note that this Gaussian size is also suitable for studying the other polymorphs of titania.
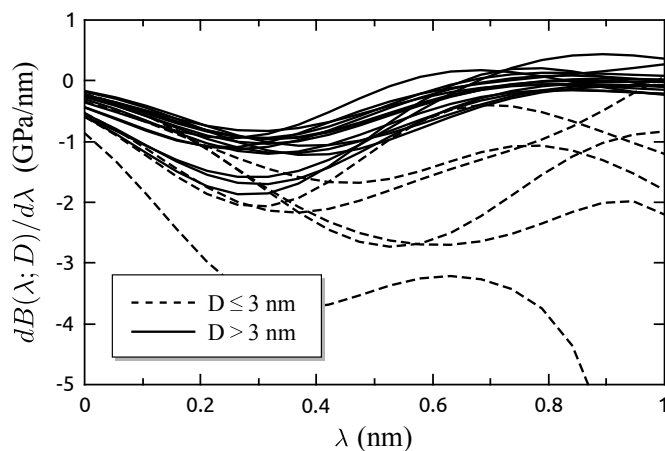
Fig. 2 The derivative of the bulk stress as a function of the 'surface thickness' λ for all twenty-one nanoparticles. Those with diameters below 3 nm have been distinguished from the rest.

Fig. 3 The bulk stresses for all twenty-one nanoparticles. The measurements for different surface thicknesses (λ) are shown with plus signs, while the best-guess $\lambda = 0.7$ nm is shown with circles. The experimental measurements were taken from Zhang et al[36].

2.2 Bulk and surface stress

Twenty-one charge-neutral nanoparticles ranging from 2 to 6 nm in diameter were constructed and then relaxed using molecular dynamics simulation. The details of the simulation method are presented in the Methodology section below.

To compute the bulk and surface stress of the nanoparticles it is necessary to identify the region where the surface ends and the bulk begins. Let us suppose that this delimitation occurs at a distance λ from the outermost atoms, then the bulk stress for a nanoparticle of diameter D, denoted $B(\lambda;D)$, is obtained by averaging $\frac{1}{3}\text{Tr}(\mathbf{\Pi}(\boldsymbol{r}))$, the hydrostatic stress field, over a concentric sphere of diameter $D - 2\lambda$. The choice of λ is somewhat arbitrary but an ideal choice would be one where the measure of the bulk stress is insensitive to small variations in λ, *i.e.* $dB(\lambda;D)/d\lambda \approx 0$. This derivative is plotted in Figure 2 as a function of λ for each nanoparticle. Curves for the nanoparticles with diameters $D \leq 3$ nm have been distinguished from the rest to illustrate that they do not level off to (approximately) zero whereas nanoparticles with $D > 3$ nm do. In particular, the curves corresponding to the larger nanoparticles begin to level off in the range $0.5 \leq \lambda \leq 0.9$ nm. We have therefore computed the bulk stress $B(\lambda;D)$ of each nanoparticle for multiple λ within this interval, specifically $\lambda = 0.5, 0.55, \ldots, 0.9$ nm, and present the results in Figure 3 (the plus symbols).

It can be seen that below 3 nm the bulk stresses are scattered and therefore highly sensitive to λ, whereas we obtain fairly consistent measures above this range. This result can be explained in light of Figure 2 which suggests that it is not meaningful to distinguish the bulk from the surface in nanoparticles with diameters smaller than 3 nm. In other words, below this size, a nanoparticle is essentially just a surface.
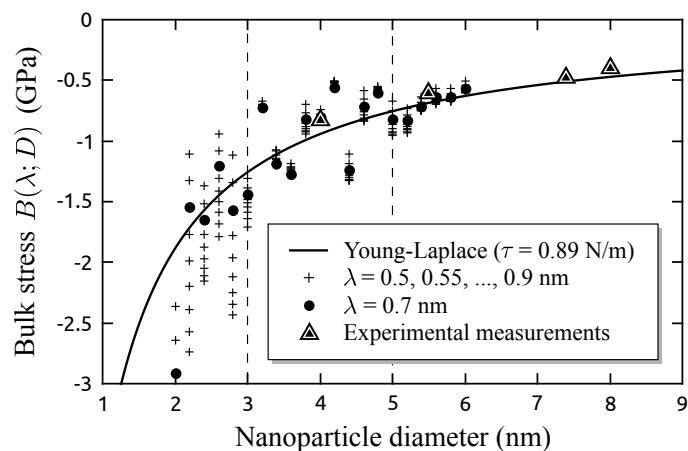
In the case of a continuous spherical nanoparticle, the bulk stress is described by the Young-Laplace equation

$$B(\lambda;D) = -\frac{4\tau(\lambda)}{D} \tag{5}$$

where $\tau(\lambda)$ is the surface stress and will depend upon the choice of λ. We fit this equation to our $B(\lambda;D)$ data points for the aforementioned range of λ but restricted the analysis to nanoparticles larger than 3 nm. The value $\lambda = 0.7$ nm was found to give the smallest variance with respect to the theoretical curve and is thus taken as the appropriate surface thickness. The corresponding surface stress is $\tau(0.7\,\text{nm}) = 0.89$ N/m which agrees with the experimental value of 0.85 ± 0.15 N/m, validating our approach.

We wish to emphasize that our 'surface thickeness' λ is merely a parameter of the analysis, chosen in order to maximize agreement with the theoretical curve. It will inevitably be larger than the actual physical thickness of the surface layer due to the fact that we are blurring the stress field (by convoluting the atomic virials with Gaussians) and thus the stress from the surface will manifest itself slightly beyond any physical strain. However, Figure 2 does provide a means of approximating the physical surface thickness: a reasonable point of demarcation between the surface and bulk would correspond to zero curvature of the stress $B(\lambda;D)$, i.e. $d^2B(\lambda;D)/d\lambda^2 = 0$, which corresponds to the minima that occur at approximately 0.3 nm (for $D > 3$ nm) in Figure 2. This value is consistent with previous estimates of surface thickness in nanoparticles[38,44,45].

As shown in Figure 3, in the interval $3 < D < 5$ nm, the bulk stresses are widely scattered about the theoretical curve. Above this range, however, the data points converge
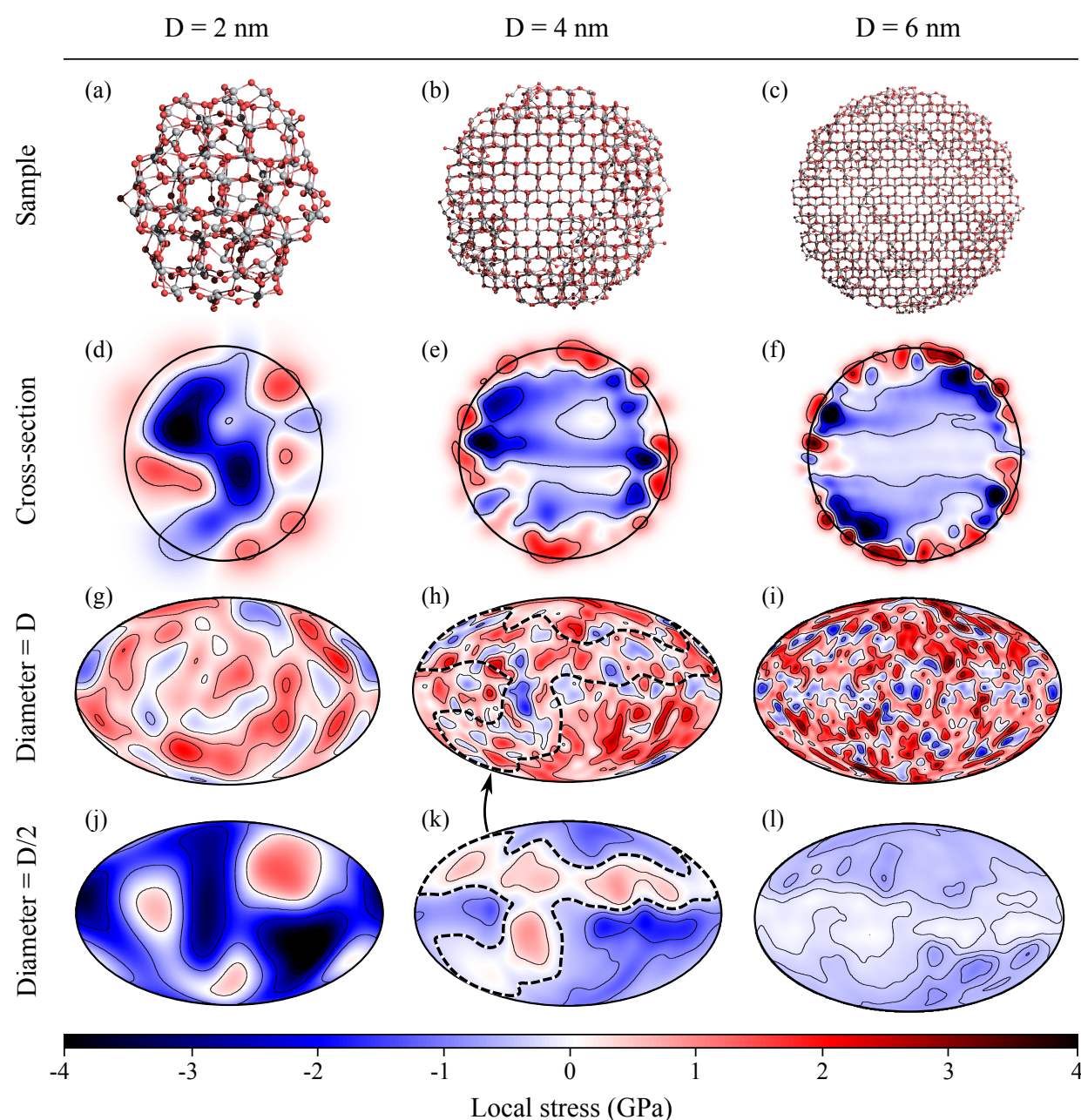
Fig. 4 The three columns each correspond to a nanoparticle, shown in the top row (a)-(c). Row (d)-(f) shows a cross-sectional plot of the stress. Rows (g)-(i) and (j)-(l) show equal-area projections of the stress on the surface of a sphere of diameter D and $D/2$, respectively. The colours correspond to the legend at the bottom.

towards the theoretical curve. This implies that the atomistic-continuum threshold for describing spherical titania nanoparticles is about 5-6 nm. We can rationalize this transition by considering the distribution of stress in the nanoparticles.

2.3 Stress distribution

Figure 4 shows three nanoparticles, (a)-(c), of respective diameters 2, 4, and 6 nm. Each column depicts the corresponding stress field. Figures (d)-(f) show cross-sectional plots of the stresses, while the remaining two rows are Mollweide equal-area projections of the stress on the surface of concen-

tric spheres of diameters D and $D/2$, respectively. In other words, they show the equiradial stress distribution ((g)-(i)) on the surface, and ((j)-(l)) in the core, of each nanoparticle. It is important to note that one can only speak very loosely of "stress" in the vicinity of the surface (or any other inhomogeneity). Nevertheless, as is expected from the virial definition itself, and as will be demonstrated in this section, the "stress" in the surface region does provide qualitative information regarding the magnitude and nature of the forces (*e.g.,* compressive or expansive).

The surfaces can be seen to display significant stress inhomogeneities that include substantial patches of negative surface stress. Such inhomogeneities are, of course, expected given the large structural variations on the surface. The bulk stresses, on the other hand, also exhibit surprisingly large inhomogeneities. These must be a consequence of the surface inhomogeneities. Indeed, a surface-bulk stress correlation can be identified quite easily by comparing the equiradial stress at the surface (h) with that in the core (k) for the 4 nm nanoparticle. For this purpose, we have traced a contour in (k) and superimposed it upon the surface (h). In the core (k), the contour primarily encloses regions of positive stress, with the negative stress excluded. In contrast, at the surface, the patches of negative surface stress fall almost invariably within the correlative region of the contour. It follows that the negative regions of the surface must undergo local expansion which result in the local bulk being stretched, thus generating positive stress. We conclude that, around this particle size (roughly $3 < D < 5$ nm), surface distortions induce large bulk inhomogeneities that cause the continuum model to fail.

Finally, we note that in the smallest (2 nm) nanoparticle (d), it is visually apparent that there is no meaningful way to delimit the bulk from the surface. This explains why we could not quantify the bulk stress with any consistency below 3 nm.

The visualisation of stress showcased here may prove valuable given recent advances in experimental methodologies that enable the imaging of strain distribution in nanomaterials[46–50].

2.4 Charge-induced stress

We can predict the bulk stress induced by a surface charge in a continuum model by considering a continuous spherical particle for which the bulk stress is zero at a diameter D_0 and the equilibrium diameter is D. By minimising the energy of such a particle it can be shown that

$$\kappa \left(\frac{D^3}{D_0^3} - 1 \right) = -\frac{4\tau}{D} + \frac{1}{2\varepsilon_0} \left(\frac{Q}{\pi D^2} \right)^2 \qquad (6)$$

where τ is the surface stress, Q the net surface charge, κ the bulk modulus, and ε_0 the permittivity of free space. This equation describes the balancing of stress in the particle, with the
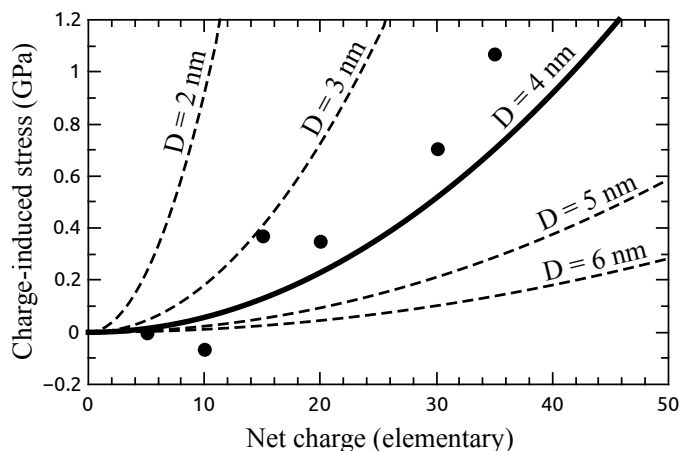
Fig. 5 The change in bulk stress due to an excess charge adsorbed on the surface. The measurements were made for a 4 nm nanoparticle (circles). The corresponding theoretical predictions are shown with the solid line.

term on the left-hand side being equal to the bulk stress. The first term on the right-hand side is the stress exerted by the surface on the bulk, in accord with the Young-Laplace equation, and the final term is, effectively, the stress exerted on the bulk by a net and uniform surface charge Q.

To test the validity of this simple model in describing discrete charges distributed almost uniformly across a nanoparticle, we placed an excess number of oxygen ions onto the surface of the 4 nm nanoparticle. At sufficiently high temperatures the surfaces of such nanoparticles would reconstruct to minimize the electrostatic energy but this option is inhibited at low temperatures due to high activation barriers. In the absence of reconstruction the nanoparticles expand to reduce the electrostatic self-interaction of the surface charge. We therefore relaxed the charged nanoparticles at 10 K to inhibit reconstruction and investigate the bulk stress induced by surface charge. We believe such simulations are relevant to the scenario of charged organic molecules adsorbed on the surfaces of nanoparticles since, in these cases, reconstruction would be unlikely to occur.

The resultant changes in bulk stress for varying charge densities are presented in Figure 5 (circles) along with the theoretical curves (Equation (6)). For the smaller charge densities the data points do not follow the predicted trend, which is not surprising since they fall far short of the assumption of uniformity. However, for the larger charge densities, where the assumption of uniformity is more legitimate, the stresses agree reasonably well with the theory, giving very similar magnitudes and displaying the correct charge-dependence. The discrepancy between the data points and the theoretical curve is likely due to the assumptions of uniformity, continuity, and perfect sphericity. Another cause could be the effect that the

added ions have on surface structure which will affect the surface stress, and therefore the bulk stress.

In any case, the magnitude of the charge-induced stress is surprisingly large (up to 1 GPa). An excess charge could therefore reduce or even eliminate the compression caused by the surface stress in nanoparticles, and may therefore provide a means of engineering strain at the nanoscale.

3 Conclusions

We have introduced a method for studying stress in nanoparticles of both single- and multi-component materials and applied it to titania.

We have demonstrated that the surface stress induces a stress in the interior of the nanoparticle, the magnitude of which increases as the diameter of the particle decreases. For particles with diameters larger than 5 nm the calculated bulk stresses agree well with experimental measurements. Fitting the results to the Young-Laplace relationship gives a value of 0.89 N/m for the surface stress, in agreement with the experimental value of 0.85 ± 0.15 N/m. This agreement validates the use of atomistic simulation as an alternative to experimentation for studying stress and strain in nanoparticles.

Adding discrete charges to the surface of the nanoparticles induces an additional stress as the particle expands in order to decrease the Coulomb interaction, and can be reasonably well described by a continuum electrostatic/elasticity model. This charge-induced tensile stress can more than compensate for the compressive stress induced by the surface stress and suggests that the adsorption of charged molecules on nanoparticle surfaces may prove to be a viable technique for stress-induced band structure engineering.

Thus our investigation has provided new insight into the effects of surface stress at an atomic level. It could easily be applied to other important technological nanostructured materials and make a real contribution to stress/strain-induced band gap engineering in quantum dots and semiconductor devices.

4 Methodology

4.1 Atomic-level stress: basic theory

The total stress tensor of an atomic system of volume Ω is equal to the volume-average of the constituent atomic virials,

$$\Pi^{\alpha\beta} = \frac{1}{\Omega} \sum_i \mathscr{W}_i^{\alpha\beta} \qquad (7)$$

where, for the two-body interatomic potentials $\phi_{ij}(r)$, the i-th atomic virial is

$$\mathscr{W}_i^{\alpha\beta} = -m_i v_i^\alpha v_i^\beta - \frac{1}{2} \sum_{j\neq i} \left(-\frac{1}{r_{ij}} \frac{\partial \phi_{ij}(r_{ij})}{\partial r} \right) r_{ij}^\alpha r_{ij}^\beta + \dots \quad (8)$$

where $\mathbf{r}_i$ and $\mathbf{v}_i$ are the position and velocity vectors of atom i respectively, and $\mathbf{r}_{ij} = \mathbf{r}_i - \mathbf{r}_j$. The superscripts denote the Cartesian components and the ellipsis represents the higher-order atomic virial contributions that may arise in molecular simulation, such as three- and four-body interactions and a k-space term from long-range electrostatics.

For an appropriate atomic volume ω_i, such as the Wigner-Seitz/Voronoi volume, the atomic virial stress of the i-th atom can be defined thus, $\pi_i^{\alpha\beta} = \mathscr{W}_i^{\alpha\beta}/\omega_i$. This quantity is taken to be a measure of the stress contributed by, and therefore incident upon, the i-th atom. At any instant in time it can be decomposed into three parts

$$\boldsymbol{\pi}_i = \boldsymbol{\pi}_i^{\text{cauchy}} + \boldsymbol{\pi}_i^{\text{thermal}} + \boldsymbol{\pi}_i^{\text{unphysical}} \qquad (9)$$

The first term is the Cauchy stress tensor which is the physically-meaningful component that we are interested in computing. The second term is noise caused by thermal fluctuations: as the atoms oscillate they produce momentary strains and thus stresses. These thermal stresses can be eliminated through temporal averaging. The remaining— unphysical—term is essentially a mathematical artifact. In single-component materials it is zero due to symmetry. In ionic materials, however, this species-dependent term is typically on the order of 10 GPa and therefore obfuscates the Cauchy stress. Fortunately though, by definition, the unphysical terms must cancel and disappear when averaged over a sufficiently large volume, *i.e.* they can be eliminated through local spatial averaging.

If we define a continuous, non-negative function $\mathscr{P}(\mathbf{r})$ such that $\int_\Omega \mathscr{P}(\mathbf{r})\,d\mathbf{r} = 1$, then the total stress tensor of Equation (7) can be rewritten as follows

$$\Pi^{\alpha\beta} = \frac{1}{\Omega} \sum_i \left(\int_\Omega \mathscr{P}(\mathbf{r} - \langle\mathbf{r}_i\rangle)\,d\mathbf{r} \right) \langle\mathscr{W}_i^{\alpha\beta}\rangle \qquad (10)$$

$$= \frac{1}{\Omega} \int_\Omega \left(\sum_i \mathscr{P}(\mathbf{r} - \langle\mathbf{r}_i\rangle)\langle\mathscr{W}_i^{\alpha\beta}\rangle \right) d\mathbf{r} \qquad (11)$$

from which a continuous Cauchy stress field is recovered

$$\Pi^{\alpha\beta}(\mathbf{r}) = \sum_i \mathscr{P}(\mathbf{r} - \langle\mathbf{r}_i\rangle)\langle\mathscr{W}_i^{\alpha\beta}\rangle \qquad (12)$$

where $\langle\cdot\rangle$ denotes time-averaging and is performed to eliminate the thermal stress field. This expression matches that presented in Ref[33] and forms the basis of our stress calculations.

4.2 Constructing spherical nanoparticles

Spherical nanoparticles were constructed by cutting spheres of the desired diameters from an infinite lattice of anatase. This straightforward method of constructing spherical nanoparticles is common in atomistic studies of nanoparticles (*e.g.*,

Refs[51–54]). We neutralized each nanoparticle by randomly removing any excess ions from their surfaces.

4.3 Molecular dynamics simulations

The molecular dynamics simulations were performed using DL_POLY Classic 1.9[55] that was modified to compute and output the atomic virials of Equation (8). Each nanoparticle was relaxed for 0.1 ns at 300 K to allow the surfaces to reconstruct. They were then quenched at 10 K and equilibrated for 1 ns, allowing mechanical equilibrium to be achieved while minimising thermal fluctuations. This was followed by a further 0.1 ns production period during which time the atomic virials and coordinates were averaged.

The simulations were performed in the canonical ensemble. Each nanoparticle was in a non-periodic (infinite) volume and the electrostatics were computed directly with a 7 nm cutoff. In the bulk simulations, the long-range electrostatics were handled by the Ewald summation. The Nosé-Hoover thermostat maintained the desired temperature with a relaxation constant of 0.5 ps. The leapfrog Verlet algorithm with a time-step of 4 fs was used to integrate the equations of motion. The titania was modelled using the force field of Matsui and Akaogi[56] which is considered the most suitable titania force field for use in molecular dynamics simulations[57–59], and consists of pairwise Buckingham and Coulomb potentials.

Acknowledgements

References

1 L. Thulin and J. Guerra, *Physical Review B*, 2008, **77**, 195112.

2 *Journal of Applied Physics*, 1983, **54**, 2052–2056.

3 D. Zhao, S. Xu, M. Xie, S. Tong and H. Yang, *Applied physics letters*, 2003, **83**, 677–679.

4 T. Takeuchi, H. Takeuchi, S. Sota, H. Sakai, H. Amano and I. Akasaki, *JAPANESE JOURNAL OF APPLIED PHYSICS PART 2 LETTERS*, 1997, **36**, L177–L179.

5 A. M. Smith and S. Nie, *Accounts of chemical research*, 2009, **43**, 190–200.

6 D. Brasen, E. A. Fitzgerald Jr, M. L. Green and Y.-h. Xie, *Method for making low defect density semiconductor heterostructure and devices made thereby.*, 1992, EP Patent 0,514,018.

7 D. Brasen, E. A. Fitzgerald Jr, M. L. Green, D. P. Monroe, P. J. Silverman and Y.-H. Xie, *Semiconductor heterostructure devices with strained semiconductor layers*, 1995, US Patent 5,442,205.

8 T. Detchprohm, K. Hiramatsu, K. Itoh and I. Akasaki, *Japanese journal of applied physics*, 1992, **31**, L1454–L1456.

9 C. Yuan, Q. Liu and B. Xu, *The Journal of Physical Chemistry C*, 2011, **115**, 16374–16377.

10 M. J. Walsh, K. Yoshida, A. Kuwabara, M. L. Pay, P. L. Gai and E. D. Boyes, *Nano letters*, 2012, **12**, 2027–2031.

11 C. L. Johnson, E. Snoeck, M. Ezcurdia, B. Rodríguez-González, I. Pastoriza-Santos, L. M. Liz-Marzán and M. J. Hÿtch, *Nature materials*, 2007, **7**, 120–124.

12 S. Patala, L. D. Marks and M. Olvera de la Cruz, *The Journal of Physical Chemistry C*, 2013.

13 W. Zhang, Y. Liu, R. Cao, Z. Li, Y. Zhang, Y. Tang and K. Fan, *Journal of the American Chemical Society*, 2008, **130**, 15581–15588.

14 J. Diao, K. Gall and M. L. Dunn, *Nature Materials*, 2003, **2**, 656–660.

15 M. Haftel and K. Gall, *Physical Review B*, 2006, **74**, 035420.

16 E. Lidorikis, M. E. Bachlechner, R. K. Kalia, A. Nakano, P. Vashishta and G. Z. Voyiadjis, *Physical review letters*, 2001, **87**, 086104.

17 J. Zimmerman, E. WebbIII, J. Hoyt, R. Jones, P. Klein and D. Bammann, *Modelling and Simulation in Materials Science and Engineering*, 2004, **12**, S319.

18 J. Lutsko, *Journal of applied physics*, 1988, **64**, 1152–1154.

19 A. Machová, *Modelling and Simulation in Materials Science and Engineering*, 2001, **9**, 327.

20 J. Cormier, J. Rickman and T. Delph, *Journal of Applied Physics*, 2001, **89**, 99–104.

21 A. K. Subramaniyan and C. Sun, *International Journal of Solids and Structures*, 2008, **45**, 4340–4346.

22 Z. Sun, X. Wang, A. Soh and H. Wu, *Modelling and Simulation in Materials Science and Engineering*, 2006, **14**, 423.

23 D. Tsai, *The Journal of Chemical Physics*, 1979, **70**, 1375.

24 R. Xu and B. Liu, *Acta Mechanica Solida Sinica*, 2009, **22**, 644–649.

25 M. Zhou, *Proceedings of the Royal Society of London. Series A: Mathematical, Physical and Engineering Sciences*, 2003, **459**, 2347–2392.

26 A. Cao and Y. Wei, *Physical Review B*, 2006, **74**, 214108.

27 H. Van Swygenhoven and P. Derlet, *Physical Review B*, 2001, **64**, 224105.

28 A. Cao, Y. Wei and S. X. Mao, *Applied physics letters*, 2007, **90**, 151909–151909.

29 K. Gall, J. Diao and M. L. Dunn, *Nano Letters*, 2004, **4**, 2431–2436.

30 J.-W. Kang and H.-J. Hwang, *Nanotechnology*, 2001, **12**, 295.

31 J. Schiøtz, T. Vegge, F. Di Tolla and K. W. Jacobsen, *Physical Review B*, 1999, **60**, 11971.

32 A. Dalis and S. K. Friedlander, *Nanotechnology*, 2005, **16**, S626.

33 P. S. Branicio and D. J. Srolovitz, *Journal of Computational Physics*, 2009, **228**, 8467–8479.

34 R. J. Hardy, *The Journal of Chemical Physics*, 1982, **76**, 622.

35 S. M. Gupta and M. Tripathi, *Chinese Science Bulletin*, 2011, **56**, 1639–1657.

36 H. Zhang, B. Chen and J. Banfield, *Phys. Chem. Chem. Phys.*, 2009, **11**, 2553–2558.

37 I. Djerdj, A. Tonejc and A. Tonejc, *Electron Crystallography: Novel Approaches for Structure Determination of Nanosized Materials*, 2004.

38 V. Swamy, L. S. Dubrovinsky, N. A. Dubrovinskaia, A. S. Simionovici, M. Drakopoulos, V. Dmitriev and H.-P. Weber, *Solid state communications*, 2003, **125**, 111–115.

39 X. Li, Y. Qu, G. Sun, D. Jiang and X. Ouyang, *Journal of Physics and Chemistry of Solids*, 2007, **68**, 2405–2410.

40 A. Tonejc, I. Djerdj and A. Tonejc, *Materials Science and Engineering: C*, 2002, **19**, 85–89.

41 B. A. Morales, O. Novaro, T. Lopez, E. Sanchez and R. Gomez, *Journal*

of materials research, 1995, **10**, 2788–2796.

42 D. Lee, Z. Gemici, M. F. Rubner and R. E. Cohen, *Langmuir*, 2007, **23**, 8833–8837.

43 D. Lee, M. F. Rubner and R. E. Cohen, *Nano letters*, 2006, **6**, 2305–2312.

44 V. V. Hoang, *The Journal of Physical Chemistry B*, 2007, **111**, 12649–12656.

45 W. Sun, Q. Zeng and A. Yu, *Langmuir*, 2013, **29**, 2175–2184.

46 I. Robinson and R. Harder, *Nature materials*, 2009, **8**, 291–298.

47 J. Clark, L. Beitra, G. Xiong, A. Higginbotham, D. Fritz, H. Lemke, D. Zhu, M. Chollet, G. Williams, M. Messerschmidt *et al.*, *Science (New York, NY)*, 2013.

48 M. Watari, R. A. McKendry, M. Vögtli, G. Aeppli, Y.-A. Soh, X. Shi, G. Xiong, X. Huang, R. Harder and I. K. Robinson, *Nature Materials*, 2011, **10**, 862–866.

49 M. Couillard, G. Radtke and G. A. Botton, *Philosophical Magazine*, 2013, 1–18.

50 Y. Kim, H. Park, K. Kim, C. Kim, W. Yun, J. Lee and M. Kim, *Applied Physics Letters*, 2009, **95**, 033112–033112.

51 P. Naicker, P. Cummings, H. Zhang and J. Banfield, *The Journal of Physical Chemistry B*, 2005, **109**, 15243–15249.

52 E. Rabani, *The Journal of Chemical Physics*, 2001, **115**, 1493.

53 H. Zhang, F. Huang, B. Gilbert and J. F. Banfield, *The Journal of Physical Chemistry B*, 2003, **107**, 13051–13060.

54 H. Zhang, B. Gilbert, F. Huang and J. F. Banfield, *Nature*, 2003, **424**, 1025–1029.

55 I. T. Todorov, W. Smith, K. Trachenko and M. T. Dove, *Journal of Materials Chemistry*, 2006, **16**, 1911–1918.

56 M. Matsui and M. Akaogi, *Molecular Simulation*, 1991, **6**, 239–244.

57 D. Collins and W. Smith, *Evaluation of TiO2 Force Fields*, Cclrc technical report dl-tr-96-001, daresbury laboratory, uk technical report, 1996.

58 V. Swamy, J. Gale and L. Dubrovinsky, *Journal of Physics and Chemistry of Solids*, 2001, **62**, 887–895.

59 V. Swamy and J. Gale, *Physical Review B*, 2000, **62**, 5406.

The size-dependent surface and bulk stresses intrinsic to titania nanoparticles are investigated using atomistic simulation. Surface charge is also shown to induce a significant tensile stress.

1